Journal of Bioenergetics and Biomembranes, Vol. 32, No. 6, 2000

Modulation of the Voltage-Dependent Anion Channel (VDAC) by Glutamate[1]

Dan Gincel,[2] Shai D. Silberberg,[2] and Varda Shoshan-Barmatz[2,3]

Received March 15, 2000; accepted August 27, 2000

The voltage-dependent anion channel (VDAC), also known as mitochondrial porin, is a large channel permeable to anions, cations, ATP, and other metabolites. VDAC was purified from sheep brain synaptosomes or rat liver mitochondria using a reactive red-agarose column, in addition to the hydroxyapatitate column. The red-agarose column allowed further purification (over 98%), concentration of the protein over ten-fold, decreasing Triton X-100 concentration, and/or replacing Triton X-100 with other detergents, such as Nonidet P-40 or octylglucoside. This purified VDAC reconstituted into planar-lipid bilayer, had a unitary maximal conductance of 3.7 ± 0.1 nS in 1 M NaCl, at 10 mV and was permeable to both large cations and anions. In the maximal conducting state, the permeability ratios for Na^+, acetylcholine$^+$, dopamine,$^+$ and glutamate$^-$, relative to Cl^-, were estimated to be 0.73, 0.6, 0.44, and 0.4, respectively. In contrast, in the subconducting state, glutamate$^-$ was impermeable, while the relative permeability to acetylcholine$^+$ increased and to dopamine$^+$ remained unchanged. At the high concentrations (0.1–0.5 M) used in the permeability experiments, glutamate eliminated the bell shape of the voltage dependence of VDAC channel conductance. Glutamate at concentrations of 1 to 20 mM, in the presence of 1 M NaCl, was found to modulate the VDAC channel activity. In single-channel experiments, at low voltages (±10 mV), glutamate induced rapid fluctuations of the channel between the fully open state and long-lived low-conducting states or short-lived closed state. Glutamate modification of the channel activity, at low voltages, is dependent on voltage, requiring short-time (20–60 sec) exposure of the channel to high membrane potentials. The effect of glutamate is specific, since it was observed in the presence of 1 M NaCl and it was not obtained with aspartate or GABA. These results suggest that VDAC possesses a specific glutamate-binding site that modulates its activity.

KEY WORDS: VDAC; Porin; ion channels; ion permeability; glutamate.

INTRODUCTION

The voltage-dependent anion channel (VDAC) of the mitochondrial outer membrane; which forms a large pore, has been purified and functionally reconstituted into a planar lipid bilayer (PLB). The conductance and ionic selectivity of reconstituted VDAC in NaCl or KCl solutions is voltage dependent (Benz, 1994; Colombini, 1994; Mannella, 1997). At small transmembrane potentials (± 10 mV), the VDAC channel is in a long-lived maximal conductance state and is more selective for anions over cations. In contrast, at large transmembrane potentials (> 40 mV), the channel converts to a lower conductance state, which is more selective for cations over anions (Benz, 1994; Colombini, 1994; Mannella, 1997). The pore diameter of mammalian VDAC was estimated to be 2.4 ± 0.08 nm for the substate (Krasilnikov *et al.*, 1996), while in the main conductance state the diame-

[1] Key to abbreviations: GABA, γ-amino *n*-butyric acid; SDS–PAGE, sodium dodecyl sulfate–polyacrylamide gel electrophoresis; VDAC voltage-dependent anion channel; PLB, planar lipid bilayer; PMSF, phenylmethylsulfonyl fluoride.

[2] Department of Life Sciences and The Zlotowski Center for Neuroscience Ben-Gurion University of the Negev, Beer-Sheva, Israel.
[3] To whom all correspondence should be addressed at email: vardasb@bgumail.bgu.ac.il

0145-479X/00/1200-0571$18.00/0

ter was estimated to be 3.0–3.8 nm (Mannella *et al.*, 1992; Guo and Mannella, 1993; Krasilnikov *et al.*, 1996). Because of its large pore, VDAC is presumed to play an important role in controlling the passage of adenine nucleotides and other metabolites in and out of the mitochondria. This presumed role of VDAC gained support from the recent observations that VDAC channels reconstituted into PLB are permeable to ATP (Rostovtseva and Colombini, 1996, 1997; Rostovtsera and Bezrukov, 1998) and to other negatively charged metabolites (Hodge and Colombini, 1997). However, its permeability to large cations, except $Tris^+$ (Benz *et al.*, 1990) was not demonstrated. Recently, we have demonstrated that VDAC is permeable to Ca^{2+} only about 2.6 times less than chloride and that VDAC possesses Ca^{2+} binding sites (Gincel *et al.*, 2000). In this paper, we demonstrate the permeability of VDAC to the large cations acetylcholine and dopamine.

The modulation of VDAC channel activity by various compounds has been demonstrated. Several synthetic polyanions, *e.g.*, Konig's polyanion, dextran sulfate and polyaspartate were shown to increase the voltage dependence of VDAC channel (Mangan and Colombini, 1987; Colombini *et al.*, 1987). Biogenic polyamines such as spermine, putrecine and spermidine, and a synthetic polyamine compound 48/80 were shown to decrease the voltage dependence of the VDAC channel (Horn *et al.*, 1998). A similar effect was reported for the organometallic hexavalent dye ruthenium red (Siadat *et al.*, 1998). Recently, however, we demonstrated the complete closure of VDAC channel by ruthenium red and that this effect was prevented by Ca^{2+} (Gincel *et al.*, 2000). NADH was shown to modulate the VDAC channel activity by influencing the probability of VDAC closure (Zizi *et al.*, 1994; Lee *et al.*, 1994). ATP has been reported to bind to human VDAC (Floker *et al.*, 1994) and to modify its channel activity (Rostovtseva and Bezrukov, 1998).

In this study, the channel activity of VDAC, purified from brain synaptosomes or liver mitochondria using a new method was characterized and its modulation by glutamate demonstrated.

EXPERIMENTAL PROCEDURES

Materials

Tris, sodium glutamate, sodium aspartate, GABA, acetylcholine chloride, dopamine chloride, HEPES, asolectin, NaCl, PMSF, leupeptin, Triton X-100, Nonidet P-40, and reactive red-agarose were purchased from Sigma Chemicals Co. Alkaline phosphatase-conjugated goat anti-mouse IgG was obtained from Promega. VDAC-monoclonal antibody prepared against the N-terminal of 31HL human porin (Babel *et al.*, 1991) (clone no. 173/045, Cat. No. 529538-B) was obtained from Cal Biochem. Hydroxyapatite (Bio-Gel HTP) was purchased from Bio-Rad and celite was obtained from the British Drug Houses (BDH).

Membrane Preparation

Synaptosomes were prepared from freshly dissected sheep brain as described previously (Huntter *et al.*, 1983), except that 0.1 mM PMSF and 0.5 μg/ml leupeptin as protease inhibitors were added to all solutions. The pellets were resuspended in sucrose buffer, frozen in liquid nitrogen, and stored at −70°C. Mitochondria were isolated from rat liver (Luo *et al.*, 1998) or brain (Basford, 1967) by standard procedures. Protein concentration was determined according to Lowry *et al.* (1951) for membranes and according to Kaplan *et al.* (1985) for purified proteins.

Purification of VDAC

Brain synaptosomal membranes or rat liver mitochondria (5–200 mg of protein) were incubated for 30 min at 25°C (at 5 mg/ml) in a solution containing 10 mM $Tris_i$, pH 7.0, 0.15 mM PMSF, 0.5 μg/ml leupeptin, and 0.2% Triton X-100. After centrifugation at 44,000 × *g* for 20 min, the pellet was resuspended at 5 mg/ml in the above solution, except that the Triton X-100 concentration was 3%. The treatment of the membranes with 0.2% Triton X-100 was carried out only with synaptosomes, since it was found to extract synaptophysin, which is copurified with VDAC in the hydroxyapatite column. After incubation for 30 min at 25°C and centrifugation at 44,000 × *g* for 30 min, the 3% Triton X-100 extract was applied to a dry hydroxyapatite/celite (2:1 w/w) column (0.1 g/mg protein) (de Pinto *et al.*, 1987) and eluted with a buffer containing 5 mM $Tris_i$, pH 6.8, and 3% Triton X-100. The VDAC-containing fractions were collected, diluted three-fold with 10 mM Tris/HCl, pH 7.3, loaded onto a reactive red-agarose column (0.1 ml/mg protein), preequilibrated with 10 mM Tris/HCl, pH 7.3, and 0.4% Nonidet P-40. The loaded column was

washed with the above buffer and VDAC was eluted at high concentration with the same buffer containing 0.3 M NaCl. The source of synaptosomal VDAC is the mitochondrial and other symaptosomal membranes (data not shown, D. Gincel *et al.*, 2000 unpublished results).

Gel Electrophoresis and Immunoblot Analyses

Analysis of the protein profile was performed using SDS–PAGE with discontinuous buffer system of Laemmli (1970) using 1.5-mm thick slab gels of 10% and 3.5% acrylamide for separating and stacking gels, respectively. Gels were stained with Coomassie Brilliant blue. Molecular weight standards were: phosphorylase *b*, 97,400; bovine serum albumin, 66,200; ovalbumin, 45,000; bovine carbonic anhydrase, 31,000; and soybean trypsin inhibitor, 21,500 (Bio-Rad).

Western blot analysis was carried out by standard procedure (Towbin *et al.*, 1979). The separated proteins from SDS–PAGE were electrophoretically transferred onto nitrocellulose membranes. For immunostaining, the membranes were blocked with 3% nonfat dry milk and 0.1% Tween-20 in Tris-buffered saline, incubated with either monoclonal anti-VDAC antibodies (1:5,000) and then with alkaline phosphatase-conjugated anti-mouse IgG as a secondary antibody (1:10,000). The color was developed (within 1 min) with 5-bromo-4-chloro-3-indolyl phosphate and nitro-blue tetrazolium.

Single-Channel Recording and Analysis

Reconstitution of VDAC into planar-lipid bilayer (PLB), single-channel current recording, and data analysis were carried out as previously described (Shoshan-Barmatz *et al.*, 1996; Shafir *et al.*, 1998a,b). Briefly, PLB were prepared from soybean asolactin, dissolved in *n*-decane (50 mg/ml). Only PLB with a resistance greater than 100 GΩ were used. Purified VDAC (about 1 ng) was added to the *cis* chamber. After one or a few channels inserted into the PLB, the excess protein was removed by washing the *cis* chamber with 20 volumes of solution to prevent further incorporation. Currents were recorded under voltage clamp using a Bilayer Clamp BC-525B amplifier (Warner Instrument Corp.). The currents were measured with respect to the *trans* side of the membrane (ground). The currents were low-pass filtered at 1 kHz (−3dB), using a Bessal filter (Frequency Devices 902), and digitized on-line using a Digidata 1200 interface board and pCLAMP 6 software (Axon Instruments, Inc.). Sigma Plot 2.0 scientific software (Jandel Scientific) was used for curve fitting. In each set of solutions, the transmembrane potential was changed linearly (voltage ramp), between −60 and +60 mV, at a rate of 62.5 mV/s in order to determine the reversal potential point.

NaCl and sodium glutamate solutions contained 10 mM Tris/HEPES. A stock solution of acetylcholine chloride (0.5 M) was prepared at a pH of 5.2 and used within 3 days. For better stability, the pH of acetylcholine chloride solutions was 6.4 (using 10 mM Tris/Mes). Dopamine chloride was prepared fresh for each experiment. All experiments were performed at 21–25°C.

The cation activity ratio in the different concentration gradients of NaCl and sodium glutamate were estimated from the equilibrium potential measured from bilayers doped with the pore-forming peptide gramicidin (0.2 ng/ml), as previously described (Hodge and Colombini, 1997). The equilibrium potentials obtained were exactly as predicted by the Nernst equation, indicating that exchanging solutions by perfusion is effective.

RESULTS

Purification of VDAC from Brain Synaptosomes

We have purified VDAC from brain synaptosomes using a two-step chromatography method: hydroxyapatite column followed by reactive red-agarose column (Fig. 1). We found that the synaptic vesicle protein synaptophysin, which copurifies with VDAC on hydroxyapatite column, can be extracted from synaptosomes with 0.2% Triton X-100 and VDAC can then be solubilized by 3% Triton X-100. Figure 1A shows that, as shown for the purification of VDAC from mitochondria, over 90% of the Triton X-100-(3%) extracted proteins applied to the hydroxyapatite column bind to the column, but the 36-kDa protein, identified by specific monoclonal antibody as VDAC, did not bind (Fig. 1B). For further purification, the VDAC-containing fractions from the hydroxyapatite column were combined and applied to a reactive red-agarose column. NaCl (0.3 M) eluted VDAC bound to the reactive red-agarose (Fig. 1B, fractions 10,11). The purity of the synaptosomal VDAC obtained by

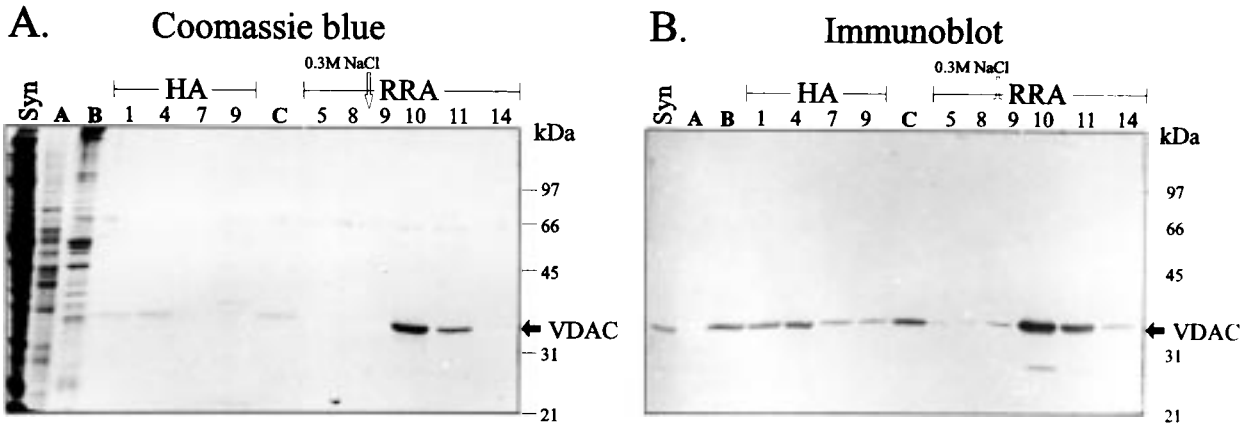

Fig. 1. Purification of VDAC from brain synaptosomes. VDAC was purified from sheep brain synaptosomes using a two-step method: hydroxyapapetite (HA) and reactive red-agarose (RRA) chromatography. Synaptosomes and VDAC were purified as described under Experimental Procedures. Synaptosomes, before (Syn) and after treatment with 0.2% Triton X-100 (A), 3% Triton X-100 extract (B), and fractions obtained from HA (1, 4, 7, and 9) and RRA (5–14) columns were subjected to SDS–PAGE (10% acrylamide) and Western blot analyses. Fractions 1 to 7 from HA column were combined (C) and applied to RRA column. The Coomassie-stained gel is shown in (A), and the corresponding immunoblot in (B). The positions of molecular weight standards (Bio-Rad) are indicated. The anti-VDAC cross-reacting band below VDAC is observed in several studies and might represent an isoform (Shoshan-Barmatz *et al.*, 1996; Shafir *et al.*, 1998a; 1998b).

this purification procedure is over 98% and this VDAC was stored at −20°C and used (up to 2 months) in single-channel reconstitution experiments presented below. By introducing the reactive-red agarose column, VDAC could not only be further purified, but also concentrated over tenfold and the Triton X-100 concentration could be reduced tenfold (to 0.3–0.4%) or exchanged with other detergents, such as 0.3% Nonidet P-40. Using the same method, VDAC was purified from rat liver and yeast mitochondria and skeletal muscle sarcoplasmic reticulum membranes.

Characterization of VDAC Activity

The purified synaptosomal VDAC was reconstituted into PLB and studied under voltage-clamp conditions. The average steady-state conductance of VDAC had a bell-shaped dependence on voltage (Fig. 2A), as found for other VDAC channels (Benz, 1994; Colombini, 1994; Shoshan-Barmatz *et al.*, 1996; Mannella, 1997; Bathori *et al.*, 1999). Each point (full circles) represents the average conductance normalized to the conductance at −10 mV, determined from four separate membrane bilayers containing at least 20 channels each. At large (>50 mV) negative or positive voltages, the average conductance was about 40% of the maximal conductance. This bell-shaped voltage dependence is similar to that obtained for VDAC isolated from brain mitochondria (open circles) and is a well-defined characteristic of VDAC (Benz, 1994; Colombini, 1994; Mannella, 1997).

Figure 2B shows six current traces from a single synaptosomal VDAC, in response to voltage steps, from a holding potential of 0 mV to the potentials indicated above each current trace. Similar to all known VDAC channels, VDAC was fully open at 0 mV, however, no net current was measured at this potential (dashed line), since symmetrical solutions were used in this experiment. The chord conductance of the main conductance state could be assessed in symmetrical solutions by applying either −10 or +10 mV to the membrane. At these relatively small membrane potentials, the conductance remained constant for up to 120 min of recording (data not shown). In symmetrical solutions of 1 M NaCl the chord conductance at 10 mV was estimated to be 3.7 ± 0.1 nS (n = 11).

In contrast to the constant currents observed at −10 or +10 mV in NaCl solutions, the channel converted to a lower conductance state within seconds when larger voltage steps were applied (Fig. 2B). These substates were identified by a rapid transition from the main conductance level to a different conductance level. The magnitude of the voltage step determined both the rate of transition into the subconductance state and the actual subconductance level. Large membrane voltage steps were followed by transitions into a subconductance level within a few seconds, while moderate voltage steps were

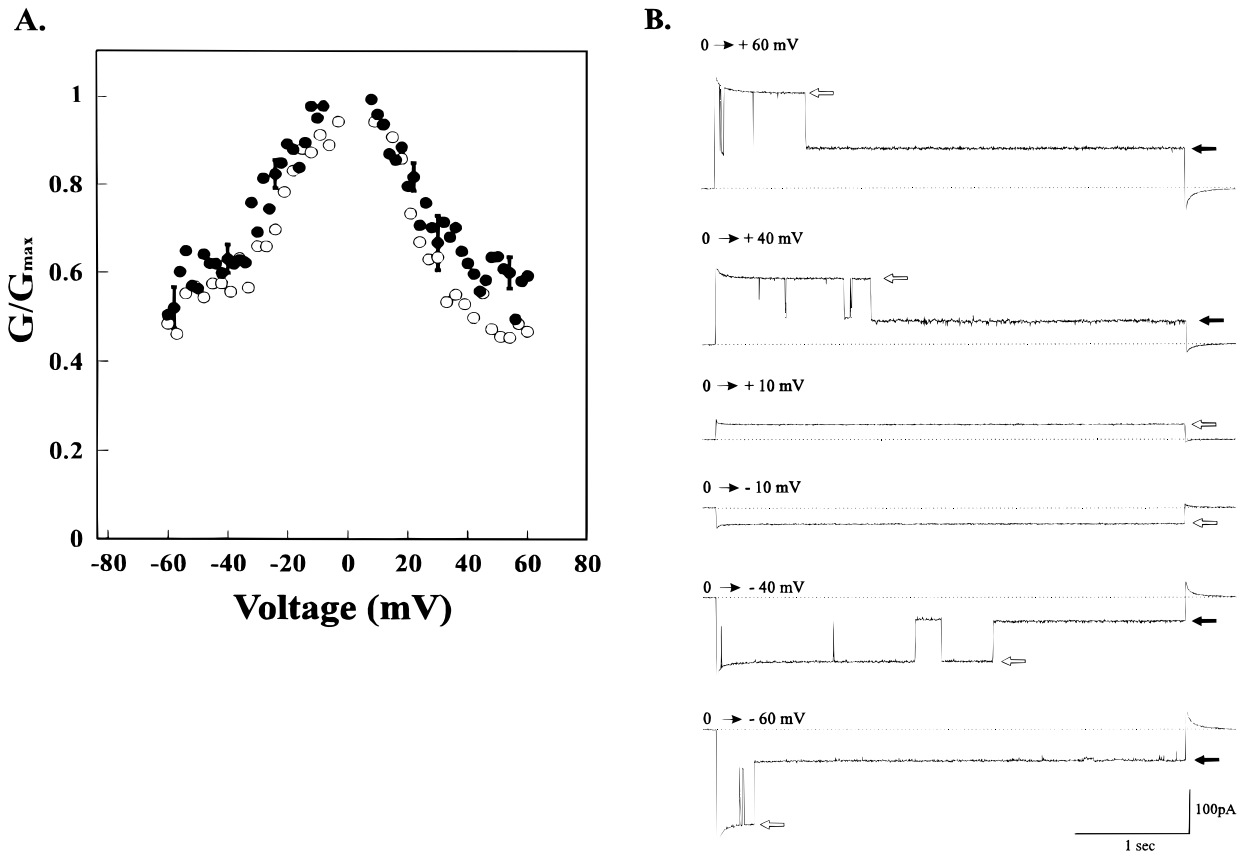

Fig. 2. Brain synaptosomal VDAC and mitochondrial VDAC have a similar voltage dependence. Purified VDAC (1 ng) was reconstituted into planar lipid bilayer (PLB) as described under Experimental Procedures. In (A), the average steady-state conductance of synaptosomal VDAC (closed circles) and brain mitochondrial VDAC (open circles) as a function of voltage was determined by measuring the average conductance of PLB containing at least 20 channels in symmetrical solutions of 1 M NaCl. The conductance (G) at a given voltage was normalized to the conductance at −10 mV (G_{max}). Each point is the average of four experiments. For clarity, only parts of the error bars (SE) are presented. In (B), current traces were obtained in response to voltage steps from 0 mV to the voltage indicated above each current trace. The dashed line indicates the zero-current level and the open and filled arrows indicate the main and subconductance states of the channel, respectively.

followed by slower transitions into higher subconductance levels. For example, at −40 and −60 mV, the chord conductance of the subconductance state was 2.0 ± 0.1 and 1.3 ± 0.1 nS (n = 3), respectively. The smaller conductance of VDAC at large transmembrane potentials most probably accounts for the bell-shaped average voltage-conductance relationship of VDAC (Fig. 2A).

Both Na^+ and Cl^- Permeate VDAC

The selectivity of VDAC for anions and cations was estimated by measuring the shifts in the zero-current potential (reversal potential) resulting from changes in the concentration gradient of NaCl. The *trans* chamber contained 150 mM NaCl, while the *cis* chamber contained either 50, 150, or 500 mM NaCl. Voltage ramps between −60 and +60 mV were used to determine the reversal potential (Fig. 3). It is well established that the selectivity of the main conductance state of mitochondrial VDAC is different from the selectivity of the subconductance state (Benz, 1994; Colombini, 1994; Mannella, 1997) Therefore, sufficiently slow voltage ramps (62.5 mV/s) were applied to assure that the transitions between the main and subconductance levels could clearly be identified. Figure 3A shows the current measured in response to a voltage ramp in symmetrical 150 mM NaCl from a bilayer containing a single VDAC channel. Transitions

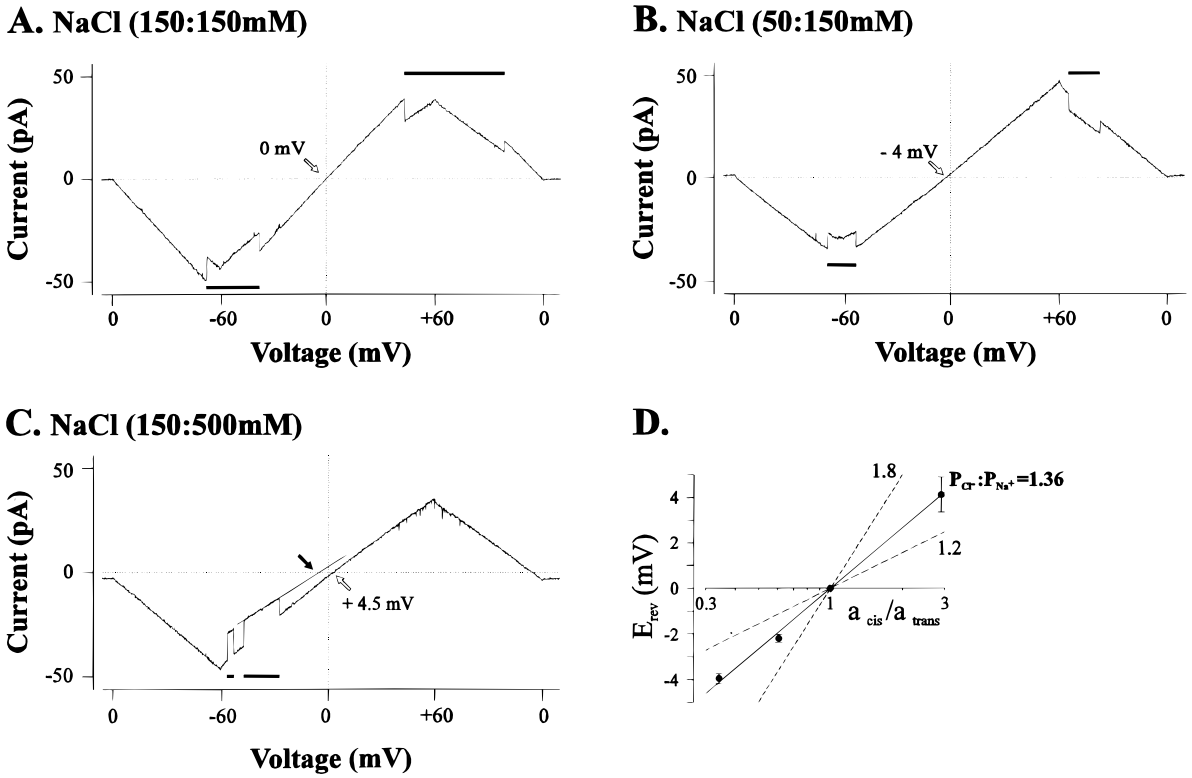

Fig. 3. Synaptosomal VDAC is permeable to both Na^+ and Cl^-. The reversal potential (potential at which current is zero) was determined by applying voltage ramps (see Experimental Procedures). The membrane voltage was changed linearly between −60 and +60 mV at 62.5 mV/s. Examples of current traces in response to voltage ramps are shown in (A), (B), and (C), in which the recording was performed in 150 mM NaCl solution on the *trans* side and either 150 (A), 50 (B) or 500 (C) mM NaCl on the *cis* side. The reversal potential (E_{rev}) obtained in each of the NaCl concentration gradient is indicated. The bars above and below the current traces indicate transitions into the subconducting state. The extrapolated linear regression of the substate is presented as a thin line in (C). The E_{rev} of the main and substates are indicated by empty and filled arrows, respectively. In (D), the E_{rev} of the main conductance state obtained at each NaCl gradient is plotted as a function of the salt activity ratio (a_c/a_t). The activity ratio of NaCl was determined as described in Experimental Procedures. Each point is the average ± SE of three to six experiments. A permeability ratio for P_{Cl}/P_{Na} of 1.36 was estimated from Eq. (1) in Results (solid line). The dashed lines represent the predicted reversal potentials, assuming ion permeability ratios of 1.2 and 1.8, as indicated.

between the main conductance state and the subconductance state are evident as abrupt changes in the current level (indicated by solid bars above and below the current trace). As expected for symmetrical solutions, the current reversed at zero mV (indicated by unfilled arrow). Reducing the concentration of NaCl in the *cis* chamber to 50 mM shifted the reversal potential to −4 mV (Fig. 3B), while raising the NaCl concentration in the *cis* chamber to 500 mM shifted the reversal potential to +4.5mV (Fig. 3C). In all solutions, the channel was in the main conductance state at the reversal potential. If the channel was permeable only to Na^+ or only to Cl^-, then with a concentration gradient of 150:50 mM the reversal potential would have shifted by approximately 27 mV (assuming an activity ratio of 2.95). The relatively small shift in reversal potential indicates that both Na^+ and Cl^- permeate VDAC. Figure 3D summarizes the dependence of the reversal potential of the main conductance state on the salt activity ratio. The permeability ratio P_{Cl}/P_{Na} was quantified by comparing the reversal potentials (E_{rev}) measured experimentally to the reversal potentials predicted by an equation, derived from the Nernst–Planck flux equations (for details, see Hodge and Colombini, 1997):

$$E_{rev} = \frac{RT}{F}\left(\frac{P_{Cl}/P_{Na} - 1}{1 + P_{Cl}/P_{Na}}\right) 1n\,\frac{a_c}{a_t} \qquad (1)$$

Where E_{rev} is the zero-current potential, R, T and F are the gas constant, the absolute temperature and Faraday constant, respectively, and a_c/a_t is the salt activity ratio

(subscript *c* and *t* denote the *cis* and *trans* chambers, respectively). The salt activity ratio was assumed to be identical to the cation activity ratio (Hodge and Colombini, 1997), which was determined experimentally by measuring the reversal potential of current through gramicidin channels incorporated into PLB (see Methods). A permeability ratio for P_{Cl^-}/P_{Na^+} of 1.36:1 was estimated from Eq. (1) and is shown as a continuous line in Fig. 3D. Predicted reversal potentials, assuming permeability ratios of 1.8:1 and 1.2:1, are also shown for comparison (dotted lines). Thus, as found for mitochondrial VDAC (Benz, 1994; Colombini 1994; Mannella, 1997), the main conductance state of synaptosomal VDAC is permeable to both cations and anions.

Large Cations also Permeate VDAC

To assess whether large cations can also permeate VDAC, experiments similar to those shown in Fig. 3 were performed using dopamine chloride and acetylcholine chloride solutions. Figure 4A and B show examples of current records in response to a voltage ramp in a concentration gradient of 150:500 mM of acetylcholine chloride or dopamine chloride solutions, respectively. Transitions between the main conductance and the suconductance state of VDAC at high voltages are clearly seen. The ability of acetycholine$^+$ and dopamine$^+$ to permeate the main conductance state of VDAC was assessed using the same experimental approach as for NaCl. The salt activity ratio of acetylcholine chloride and dopamine chloride in the different concentration gradients was assumed to be the same as the salt activity ratio of NaCl (Fig. 3). The data in Figs. 4C and D represent the average reversal potential measured at different acetylcholine chloride and dopamine chloride concentration gradients, respectively. A permeability ratio of the main conductance state for Cl^- over acetycholine$^+$ (P_{Cl^-}/P_{Ach^+}) of 1.65:1 and for Cl^- over dopamine$^+$ (P_{Cl^-}/P_{Dop^+}) of 2.3:1 were estimated from Eq. (1) and are shown as continuous lines in Fig. 4C and D, respectively. Predicted reversal potentials assuming permeability ratios of 3.0:1 and 1.2:1 are also shown for comparison (dotted lines).

The permeability of the subconductance state was estimated by linear extrapolation of the current, measured in the substate, to the zero-current potential, as illustrated for NaCl solutions in Fig. 3C (solid arrow) and for acetylcholine chloride and dopamine chloride in Fig. 4, and is summarized in Table I and discussed below.

Glutamate Permeates the VDAC Channel

Figure 5A shows an example of a current record in response to a voltage ramp in a concentration gradient of 150:500 mM of sodium glutamate solutions. Transitions between the main conductance and the subconductance state of VDAC are clearly seen. Figure 5B summarizes the dependence of the reversal potential of the main conductance state on the sodium glutamate activity ratio determined in experiments of the type shown in Fig. 3. As for the NaCl experiments, the glutamate activity was assumed to be equal to the Na^+ activity determined experimentally, using gramicidin as a cation-selective channel (see Experimental Procedures). Each point represents the average reversal potential, determined in three to four experiments. A permeability ratio for Na^+ over glutamate$^-$ (P_{Cl^-}/P_{Glu^-}) of 1.8:1 was estimated from Eq. (1) and is shown as a continuous line in Fig. 5B. Predicted reversal potentials assuming permeability ratios of 3.0:1 and 1.2:1 are also shown for comparison (dotted lines).

The voltage dependence of VDAC channel activity in the presence of 0.5 M sodium glutamate or 0.5 M NaCl solutions is shown in Fig. 5C. Surprisingly, glutamate eliminated the bell-shaped voltage-dependence of the average channel conductance (Fig. 5C), suggesting that glutamate modulates the voltage sensor of VDAC.

Glutamate Modulation of VDAC Channel Activity

To address the possible modulation of VDAC by glutamate, we tested the effect of relatively low concentrations of glutamate (1–20 mM), in the presence of 1 M NaCl on VDAC channel activity (Figs. 6 and 7). Figure 6A shows representative records of a single VDAC channel activity in symmetric solution of 1 M NaCl, before and after the addition of 5 mM glutamate. In the absence of glutamate, at 10 mV, the channel remained stable in the full conducting state for over 30 min. On the otherhand, within few seconds from the addition of glutamate (5 mM), the channel started to display relatively fast alternations between the fully open state, subconductance states, and the fully closed state (trace a, $n = 3$). In other experiments,

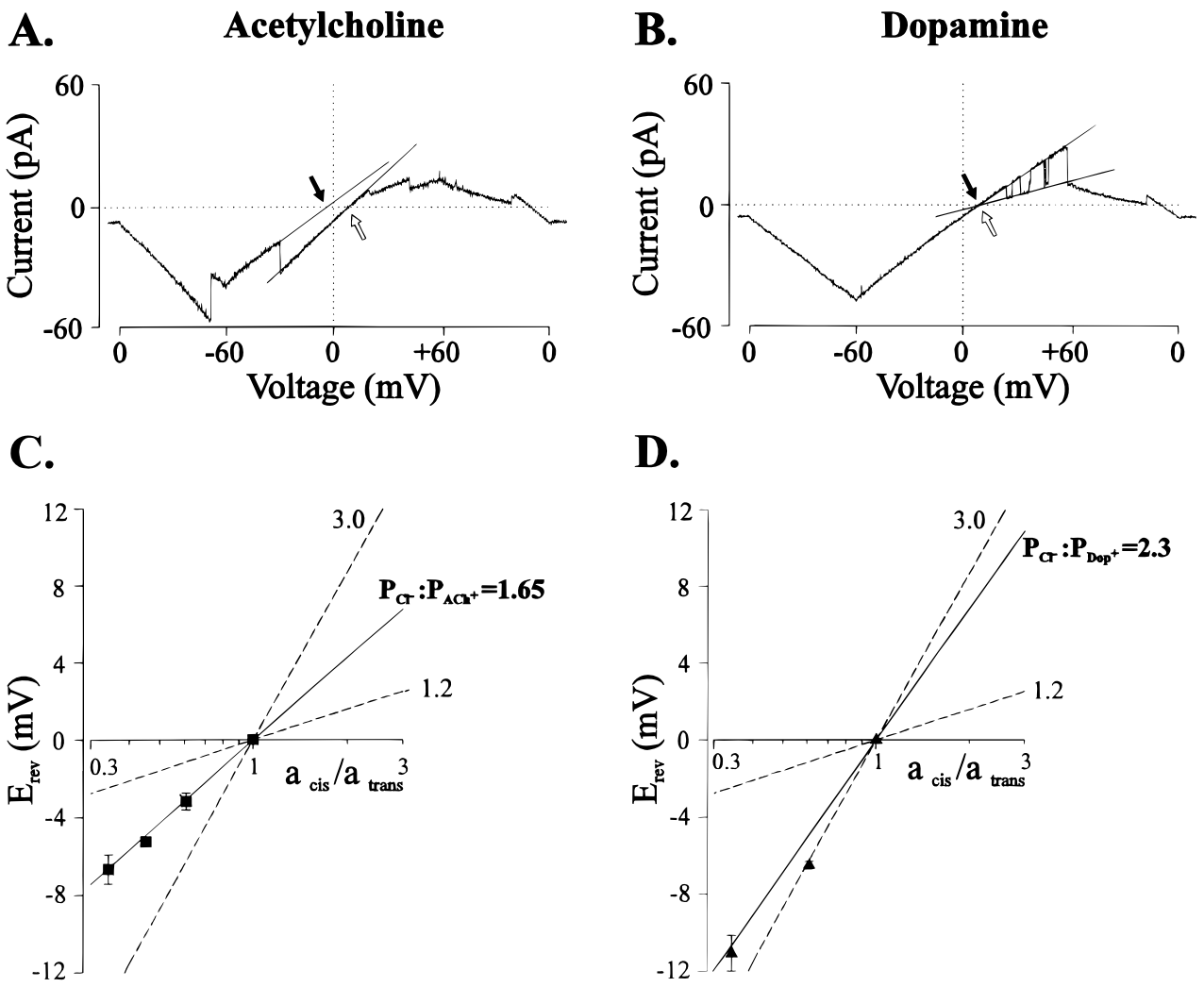

Fig. 4. VDAC is permeable to dopamine$^+$ and acetylcholine$^+$. Single VDAC channel currents in response to voltage ramps in acetylcholine chloride (A) or dopamine chloride (B) solutions. In (C) and (D), the reversal potentials for VDAC-mediated ionic currents and permeability were determined as in Fig. 3. The values shown are the mean and standard error of three to four different experiments. In each experiment, the current between −20 and +20 mV was averaged from five consecutive ramps. The reversal potentials are plotted for both dopamine$^+$ and acetylcholine$^+$ as a function of NaCl activity ratio. The dashed lines represent the predicated reversal potentials, assuming ionic permeability ratios of 1.2 or 3.0. The open and filled arrows indicate the E_{rev} of the main and substates, respectively.

the channel displayed long-lived, low-conducting states (trace b, $n = 3$). In addition, in some other experiments, the channel fluctuated between the fully open and a slightly reduced conductance state, which occasionally entered low-conducting states (trace c, $n = 2$). Modification of VDAC channel activity by glutamate was observed only when glutamate was added to the *trans* side of the bilayer (data not shown).

The effect of glutamate on VDAC channel activity was also observed in multichannel recordings (Fig. 6B). The decrease in VDAC channel conductance by glutamate (5 and 20 mM) was observed at all tested voltages but, was most pronounced at low voltages (Fig. 6B). Half-maximal inhibition of VDAC channel conductance was induced by approximately 3.8 mM of glutamate, according to a Hill decay equation (Fig. 6C). The effect of glutamate could be reversed by exchanging the solution with glutamate-free solution (data not shown).

Figure 7 shows that the onset of the effect of glutamate is voltage dependent. Addition of glutamate at a holding potential of ± 10 mV to reconstituted

Table I. Conductance and Permeability of Synaptosomal VDAC[a]

Salt solution	Main conductance			Subconductance		
	E_{rev} (mV)	G_{slope} (nS)	P_{C^+}/P_{A^-}	E_{rev} (mV)	G_{slope} (nS)	P_{C^+}/P_{A^-}
Sodium chloride	5.0 ± 0.2 (7)	1.4 ± 0.1 (4)	0.73	−9.6 ± 0.3 (6)	0.7 ± 0.1 (3)	2.1
Acetylcholine chloride	7.6 ± 0.6 (4)	0.8 ± 0.1 (2)	0.57	−2.8 ± 0.2 (5)	0.3 ± 0.1 (2)	1.2
Dopamine chloride	9.7 ± 0.4 (4)	1.3 ± 0.1 (2)	0.44	9.8 ± 0.3 (2)	0.4 ± 0.1 (2)	0.44
Sodium glutamate	−7.8 ± 0.1 (3)	0.4 ± 0.1 (3)	2.0	−23.9 ± 0.6 (8)	0.7 ± 0.1 (5)	[b]

[a] Reversal potential (E_{rev}) slope conductance (G_{slope}) and relative permeability (P_{C^+}/P_{A^-}) estimated by fitting the current in response to voltage ramps with a linear regression (see Experimental Procedures). In each of the solutions, the conductance of the main and subconductance levels were estimated with 150 mM on the *trans* side and 500 mM on the *cis* side. C^+ and A^- indicate cation and anion, respectively. The numbers are the mean ± SE and the number of experiments is indicated in parenthesis.

[b] The permeability ratio was not determined because the reversal potential was almost identical to the Nernst equilibrium potential for Na^+.

VDAC had no effect on channel activity (even after 30 min of incubation). However, when the holding potential was stepped for 20 to 60s to either +60 mV (Fig. 7A) or −60 mV (Fig. 7B), and then returned to either 10 or −10mV, glutamate induced alteration in VDAC channel activity and the channel underwent fast transitions between the open and closed or substates.

The specificity of glutamate modification of VDAC channel activity is demonstrated in Fig. 7, showing that aspartate had no effect on VDAC channel activity. Similarly GABA was without effect (data not shown). Furthermore, addition of glutamate in the presence of aspartate produced channel modification (data not shown). Glutamate modified VDAC channel activity regardless of the membranal source of VDAC—liver mitochondria or brain synaptosomes.

Permeability and Selectivity of Synaptosomal VDAC Main and Subconductance States

Table I compares the conductance and the relative permeability of the main conductance state to that of the subconductance state of synaptosomal VDAC determined in the various tested solutions, using 150:500 mM concentration gradient. The slope conductance (G_{slope}) and the reversal potential (E_{rev}) of the main and subconductance states were estimated by fitting the current with a linear regression. The slope conductance of the subconductance state was estimated only for the most frequently observed substate in each of the solutions. In all but the sodium glutamate solution, the examined solutions, the conductance in the substate was lower than in the main conductance state. However, it should be noted that occasionally in NaCl solutions, we observed a shift in the reversal potential, which was not accompanied by a change in the slope conductance. This phenomenon was not studied further. Table I also shows that, as previously reported for VDAC (Benz, 1994; Colombini, 1994; Mannella, 1997), in NaCl solutions, the subconductance state of synaptosomal VDAC has a reversed selectivity, being more permeable to Na^+ than to Cl^-. Consistent with a greater permeability of the subconductance state to cations relative to anions, acetylcholine$^+$ was more permeable than Cl^- in the substate. In contrast, dopamine$^+$ was less permeable than Cl^- in the subconductance state, and glutamate$^-$ was impermeant. Taken together, these results show that both cations and anions permeate VDAC. The permeabilities (relative to Cl^-) of Cl^-: Na^+: acetylcholine$^+$: dopamine$^+$: glutamate$^-$ of the main conductance state were estimated to be 1:0.73: 0.6: 0.44: 0.4, respectively.

DISCUSSION

We have purified VDAC from sheep brain synaptosomes and reconstituted its channel activity. The electrophysiological properties of purified synaptosomal VDAC are very similar to those reported for VDAC isolated from various other sources with respect to voltage-dependence, conductance and ion selectivity. In the main conductance state, VDAC is permeable to large anions, such as glutamate$^-$ and also to large cations such as acetylcholine$^+$ and dopamine$^+$. The permeability of VDAC to Tris$^+$ has been demonstrated (Benz *et al.*, 1990). In the subconductance state, the permeability of synaptosomal VDAC to acetylcholine$^+$ was reduced and essentially eliminated for glutamate. The finding that the conductance of the main conductance state is smaller than that of the substate in sodium

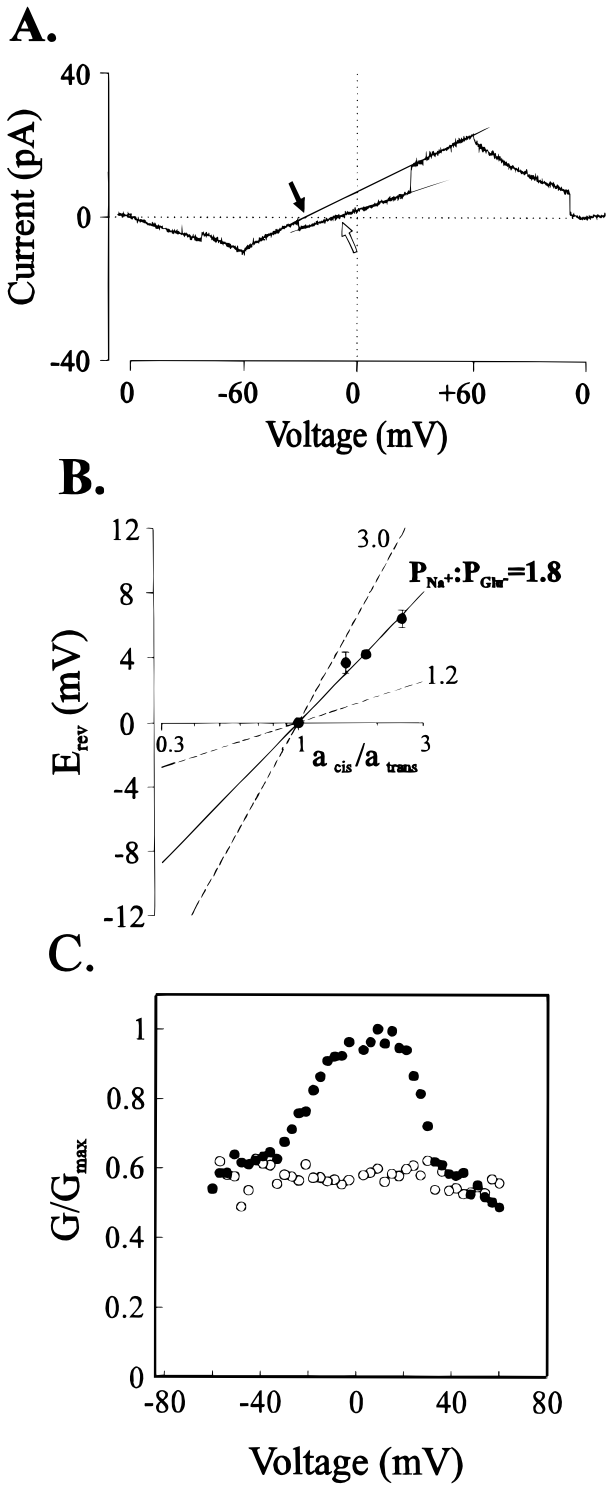

glutamate solution suggests that glutamate interfered with the passage of Na^+. This interference could result from electrostatic interactions of glutamate$^-$ with charges that line the pore of VDAC. Site-directed mutations indicated that the flow of ions through VDAC is influenced by the charge on the wall of the pore (Blachly-Dyson *et al.*, 1990). A pronounced attraction of ATP molecules to the aqueous pore of VDAC has been suggested (Rostovtsera and Bezrukov, 1998) and reversible binding of ATP to VDAC has been demonstrated (Floker *et al.*, 1994). Furthermore, the presence of binding sites for dicarboxylic anions in a VDAC-like protein in peroxisomes has been shown (Reumann *et. al.*, 1998). It is also possible that an interaction between Na^+ and glutamate$^-$ occurs within the pore, since VDAC has a large pore in which multiple ions might be present at the same time. However, the modulation of VDAC channel activity by low concentrations of glutamate demonstrated in this study suggests a direct interaction of glutamate with a specific site.

Glutamate, at relatively low concentrations, was found to modify the VDAC channel activity. Analysis of the glutamate effect on single VDAC channel activity showed that at low voltages ($\pm$10 mV) in which the channel is normally in a long-lived, fully open state, glutamates-induced rapid fluctuations of the channel between the fully open state, long-lived low-conducting states, and short-lived substate or closed state. Thus, glutamate decreases the mean channel conductance, at low negative or positive voltages, by inducing channel fluctuations between fully open and closed and/or subconductance states.

The effect of glutamate$^-$ was voltage-dependent—observed only when the channel was exposed to glutamate for a short time (20–60 s) at high (negative

Fig. 5. VDAC is permeable to and modulated by glutamate$^-$. Single VDAC channel current in response to voltage ramps in sodium glutamate solution is shown in (A); in (B), the reversal potential obtained at each sodium glutamate gradient is plotted as a function of the salt activity ratio (a_c/a_t). The activity ratio was determined as in Fig. 3. Each point is the average $\pm$ SE of three to six experiments. A permeability ratio for P_{Na^+}/P_{Glu^-} of 1.8 was estimated from Eq. (1) in Results (solid line). The dashed lines represent the predicted reversal potentials assuming ion permeability ratios of 1.2 and 3.0 as indicated. In (C), the average steady-state conductance of VDAC, relative to the maximal conductance at 10 mV, in symmetrical solutions of 0.5 M NaCl (closed circles) or after replacing the NaCl solution by 0.5 M sodium glutamate (open circles) as a function of voltage was determined by measuring the average conductance of at least 20 channels.

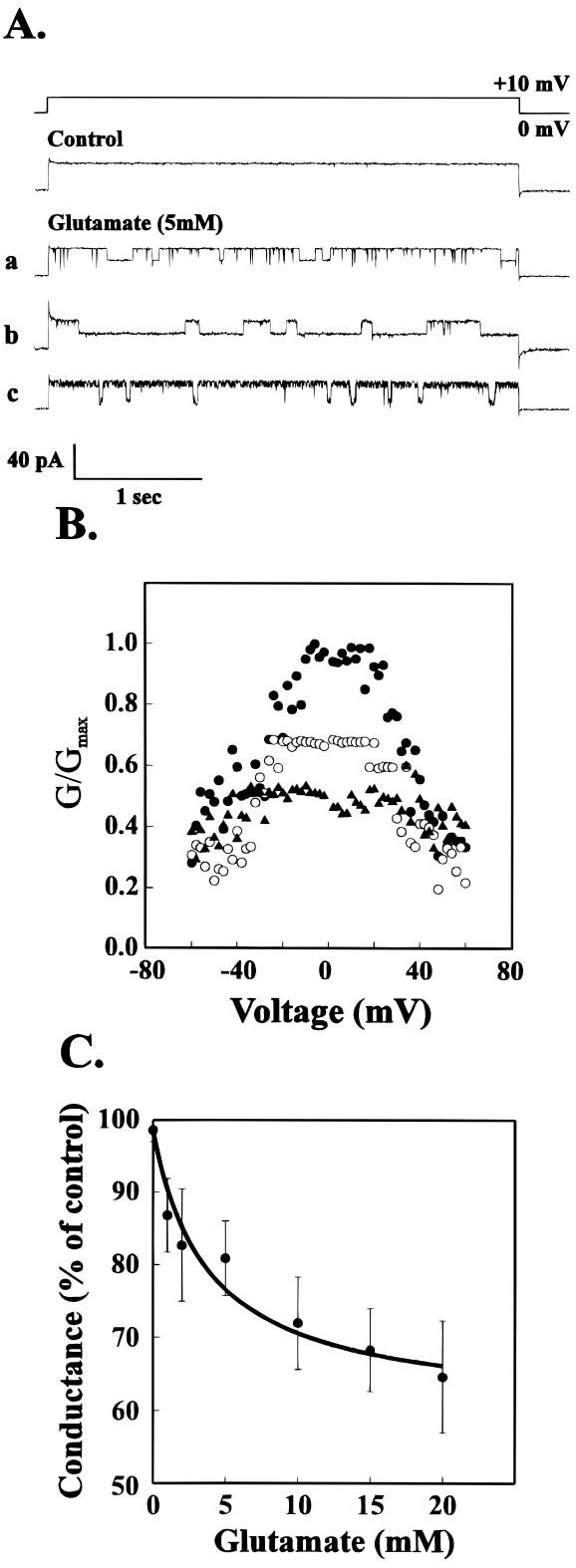

or positive) potentials. According to current view (Colombini, 1994; Benz, 1994), the multiple conductance states of VDAC correspond to different conformational states that are stabilized at the different voltages. Our results show that the effect of glutamate$^-$ is equivalent to high voltages, converting the channel into the low-conducting states even at low membrane potentials ($\pm$10 mV) (Figs. 6 and 7). This may suggest that glutamate interacts with a positively charged voltage sensor, as suggested previously for polyanions (Mangan and Colombini, 1987). However, in contrast to the asymmetric effect of polyanions (which act only when the side of the membrane to which they are applied is negative), the effect of glutamate$^-$ was obtained at both negative and positive voltages (Fig. 7). Since VDAC has two gating processes—one at positive potentials and the other at negative potentials (Zizi *et al.*, 1998)— the results suggest modification by glutamate$^-$ of both gating processes. This may result from glutamate$^-$ interacting with a single binding site that affects both gating processes or from interaction with two different binding sites. The binding site(s), however, become accessible to glutamate$^-$ at higher voltages, as indicated by the voltage dependence of the glutamate$^-$ effect on VDAC channel activity (Fig. 7).

The effect of glutamate$^-$ is specific, since it was observed in the presence of very high ionic strength (1 M NaCl) and was not mimicked by aspartate or GABA. These results suggest that VDAC possesses a specific glutamate-binding site that modulates its activity. Thus, the permeability of VDAC may be controlled not only by voltage changes, but also by glutamate and, as shown previously by associated proteins (Holden and Colombini, 1993) as well as by modulat-

Fig. 6. VDAC channel activity is modulated by glutamate. VDAC was reconstituted into PLB as in Fig. 2 and single-channel or multichannel currents through VDAC were recorded. In (A), representative single-channel records in response to a voltage step, before (control) and after the addition of 5 mM glutamate are shown (a, b, c). Multichannel (10 or more channels) recording (B) shows the relative conductance before (close circles) and after the addition of 5 (open circles) or 20 mM glutamate (closed triangle). Relative conductance was determined by dividing the conductance (G) at a given voltage by the maximal conductance (G_{max}). In (C), the data were fitted with the equation: $I/I_{max} = [\text{glutamate}]^n/([\text{glutamate}]^n + IC_{50}{}^n)$, where I is the current at 10 mV and at a given concentration of glutamate, I_{max} is the maximum current (in the absence of glutamate), IC_{50} is the concentration of glutamate that decreases the current by 50% and assuming maximal inhibition of 60%. The best fit was obtained with Hill coefficient (n) of 1.

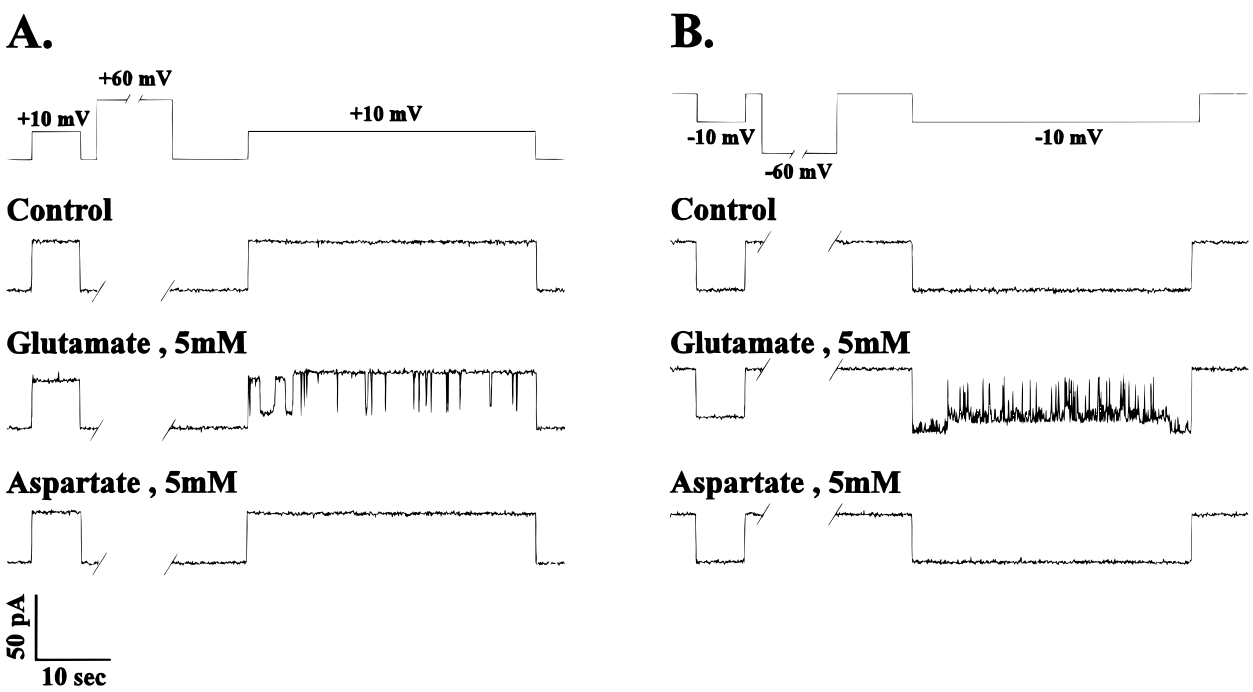

Fig. 7. Glutamate modulation of VDAC channel activity is specific and induced by high voltages. VDAC was reconstituted into PLB in the presence of 1 M NaCl as in Fig. 2. Single-channel currents through VDAC were recorded at +10 or −10mV and then, as indicated, the voltage was switched to +60 (A) or −60 mV (B) for 20 s, and, thereafter, back to +10 or −10 mV, respectively, where the channel activity was recorded. After about 5 min of recording under control conditions (at ±10 mV), glutamate (5 mM) was added and the same voltage protocol was applied. Results are representative recording from two to four different experiments. The experiment with aspartate was carried out on a different channel.

ing effectors such as NADH (Zizi *et al.*, 1994), ATP (Floker *et al.*,1994), and Ca^{2+} (Gincel *et al.*, 2000).

The interaction of glutamate$^-$ with the VDAC channel is particularly important since there is accumulating evidence that VDAC is presence in the plasma membrane (Dermietzel *et al.*, 1994; Guibert *et al.*, 1998; Reymann *et al.*, 1995; Shafir *et al.*, 1998b). However, the physiological function of VDAC in the plasma membrane and of its modulation by glutamate is not clear and will require further study.

ACKNOWLEDGMENTS

The work was supported by grants from the the Israeli Science Foundation (V. Shoshan-Barmatz).

REFERENCES

Benz, R. (1994). *Biochim. Biophys. Acta* **1197**, 167–196.
Benz, R., Kottke, M., and Brdiczka, D. (1990). *Biochim. Biophys. Acta* **1022**, 311–318.
Babel, D., Walter, G., Gotz, H., Thinnes, F. P., Jurgens, L., Konig, U., and Hilschmann, N. (1991). *Biol. Chem. Hoppe-Seyler* **372**, 1027–1034.
Basford, R. E. (1967). *Methods Enzymol.* **10**, 96–101.
Bathori, G., Parolini G., Tombola, I., Szabo, F., Messina, I., Oliva, A., De Pinto, M., Lisanti, V., Sargiacomo M., and Zoratti, M. (1999). *J. Biol. Chem.* **274**, 29607–29612.
Blachly-Dyson, E., Peng, S., Colombini, M. and Forte, M. (1990). *Science*, **247**, 1233–1236.
Colombini, M. (1994). *Current Topics Membr.* **42**, 73–101.
Colombini, M., Yeung, C. L., Tung, J., and Koeing, T. (1987). *Biochim. Biophys. Acta* **905**, 279–286.
de Pinto, V., Prezioso, G., and Palmieri, F. (1987). *Biochim. Biophys. Acta* **905**, 499–502.
Dermietzel, R., Hwang, T. K., Buettner, R., Hofer, A., Dotzler, E., Kremer, M., Deutzmann, R., Thinnes, F. P., Fishman, G., Spray, D., and Siemen, D. (1994). *Proc. Natl. Acad. Sci. USA* **91**, 499–503.
Floker, H., Thinnes, F. P., Winkelbach, H., Stadtmuller, U., Paetzold, G., Morys-Wortmann, C., Hess, D., Sternbach, H., Zimmermann, B., Kaufmann-Kolle, P., Heiden, M., Karabions, A., Reymann, S., Lalk, V. E., and Hilschmann, N. (1994). *Biol. Chem. Hoppe-Seyler* **375**, 513–520.
Gincel, D., Zaid, H., and Shoshan-Barmatz, V. (2000). *J. Biol. Chem.*, manuscript submitted.
Guibert, B., Dermietzel, R., and Sieman, D. (1998). *Intern. J. Biochem. Cell. Biol.* **30**, 379–391.
Guo, X. W. and Mannella, C.A. (1993). *Biophys. J.* **64**, 545–549.

Hodge, T. and Colombini, M. (1997). *J. Membr. Biol.* **157**, 271–279.
Holden, M. J. and Colombini, M. (1993). *Biochim. Biophys. Acta* **1144**, 396–402.
Horn, A., Reymann, S., and Thinnes, F. P. (1998). *Mol. Genet. Metab.* **63**, 239–242.
Huntter, W. B., Schiebler, W., Greengard, P., and de Camilli, P. (1983). *Cell. Biol.* **96**, 1374–1388.
Kaplan, R. S. and Pedersen, P. L. (1985). *Anal. Biochem.* **150**, 97–104.
Krasilnikov, O. V., Carneiro, C. M. M., Yuldasheva, L. N., Campos-de-Carvalho, A. C., and Nogueira, R. A., (1996). *Brazil. J. Med. Biol. Res.* **29**, 1691–1697.
Laemmli, U. K. (1970). *Nature London* **227**, 680–685.
Lee, A., Zizi, M., and Colombini, M. (1994). *J. Biol. Chem.* **269**, 30974–30980.
Lowry, O. H., Rosenbrough, N. J., Farr, A. L., and Randall, R. J. (1951). *J. Biol. Chem.* **193**, 265–275.
Luo, X., Budihardjo, I., Zou, H., Slaughter, C., and Wang, X. (1998). *Cell* **94**, 481–490.
Mangan, P. S. and Columbini, M. (1987). *Proc. Natl. Acad. Sci. USA* **84**, 4896–4900.
Mannella, C. A. (1997). *J. Bioenerg. Biomembr.* **29**, 525–531.
Mannella, C. A., Forte, M., and Colombini, M. (1992). *J. Bioenerg. Biomembr.* **24**, 7–19.
Reymann, S., Flàrke, H., Heiden, M., Jakob, C., Stadtmuller, U., Steinacker, P., Lalk, V. E., Pardowitz, I., and Thinnes, F. R. (1995). *Biochem. Mol. Med.* **54**, 75–87.
Reumann, S., Maier, E., Heldt, H. W., and Benz, R. (1998). *Eur. J. Biochem.* **251**, 359–366.
Rostovtsera, T. and Bezrukov, S. M. (1998). *Biophys. J.* **74**, 2365–2373.
Rostovtseva, T. and Colombini, M. (1996). *Biophys. J.* **72**, 1954–1962.
Rostovtseva, T. and Colombini, M. (1997). *J. Biol. Chem.* **271**, 28006–28008.
Shafir, I., Feng, W., and Shoshan-Barmatz, V. (1998a). *Eur. J. Biochem.* **253**, 627–636.
Shafir, I., Feng, W., and Shoshan-Barmatz, V. (1998b). *J. Bioenerg. Biomembr.* **30**, 499–510.
Shoshan-Barmatz, V., Hadad, N., Feng, W., Shafir, I., Orr, I., Varsanyi, M., and Heilmeyer, M. G. (1996). *FEBS Lett.* **386**, 205–210.
Siadat, S., Reymann, S., Horn, A., and Thinnes, F. P. (1998). *Mol. Genet. Metab.* **65**, 246–249.
Towbin, H., Staehelin, T., and Gordon, J. (1979). *Proc. Natl. Acad. Sci. USA* **76**, 4350–4354.
Zizi, M., Forte, M., Blachly-Dyson, E., and Colombini, M. (1994). *J. Biol. Chem.* **269**, 1614–1616.
Zizi, M., Byrd, C., Boxus, R., and Colombini, M. (1998). *Biophys. J.* **75**, 704–713.